are known to be present in the human genome (http://drnelson.utmem.edu/CytochromeP450.html). CYP enzymes that belong to families 1–3 are responsible for metabolizing clinically used drugs and xenobiotic chemicals.

In contrast, the *CYP4A* gene subfamily codes for a group of structurally and functionally conserved CYP hemoproteins that almost exclusively catalyze the ω and ω-1 hydroxylation of several saturated and polyunsaturated fatty acids and eicosanoids [1]. CYP4A11, a major isoform among humans CYP4A, is known to be expressed in the kidney and metabolizes arachidonic acid to 19- and 20-hydroxyeicosatetraenoic acid (19- and 20-HETE) [2,3]. The 20-HETE metabolite can act in either a prohypertensive or antihypertensive manner depending on its expression at renovascular or tubular sites, respectively [4–6].

Wide interindividual differences in metabolic capacity have been detected in many CYP enzymes [7]. It has been found that these phenotypic differences are partly genetically determined. Gainer et al. [8] have recently reported that a (8590T>C, Phe434Ser) *CYP4A11* variant produces a protein with a significantly reduced 20-HETE synthase activity, and in Caucasians the 8590C allele is associated with an increased prevalence of hypertension after adjustment for age, gender, and BMI in both males and females.

Kawashima et al. [9] initially reported the isolation of a *CYP4A11*-related gene. Two groups recently identified this to be *CYP4A22* that exhibits 95% identity to the *CYP4A11* on the coding region [10,11]. To our knowledge, although sequence analysis in the *CYP4A22* gene has been carried out, no polymorphism has been described. In the present study, we systematically investigated the variants of *CYP4A22* in a population sample that comprised 191 Japanese subjects. For detecting the genetic variants, we used denaturing HPLC (DHPLC) to analyze the protein-coding region of all of the 12 exons. After the variations were detected, the respective DNAs were sequenced to identify the alterations. In addition, cloning methods were used to determine these haplotypes.

2. Materials and methods

2.1. Subjects and DNA samples

Venous blood was obtained from 191 unrelated healthy Japanese volunteers and patients admitted to Tohoku University Hospital. Written informed consent was obtained from all the blood donors, and the study was approved by the Local Ethics Committee of Tohoku University Hospital and Tohoku Pharmaceutical University. DNA was isolated from K_2EDTA-anticoagulated peripheral blood by using QIAamp DNA Mini Kits (Qiagen, Hilden, Germany) in accordance with the manufacturer's instructions.

2.2. PCR amplification

Table 1 lists the primer pairs used to specifically amplify *CYP4A22* exons. These primers were designed to maximize the difference between *CYP4A22* and *CYP4A11* that were highly homologous to each other based on the genomic sequence reported in the NCBI database with accession number NT032977.7. Amplicons were generated using the AmpliTaq Gold PCR Master Mix (Applied Biosystems, Foster City, CA, USA). The thermal profile consisted of denaturation at 95 °C for 10 min, followed by 35–40 cycles of denaturation at 95 °C for 30 s, annealing at 60 °C for 30 s, extension at 72 °C for 30 s, and a final extension at 72 °C for 7 min. Heteroduplexes were then generated by means of a thermal cycler as follows: 95 °C for 1 min; 95 °C, reduced by 1.5 °C per min, for 47 cycles.

2.3. DHPLC analysis

The PCR products were analyzed using the DHPLC system, WAVE (Transgenomic Inc., Omaha, NE, USA). Unpu-

Table 1
Amplification and DHPLC conditions for *CYP4A22* SNP analysis of genomic DNA

Amplified exon	Size (bp)	Forward primer (5′ → 3′)	Reverse primer (5′ → 3′)	DHPLC temperature (°C)
1	334	gacaatcctcccatgacttaagcacaggt	tcagagccgcatccctcc	63.3
2	392	cctgctgcaaagactagaagt	catattgttttaaacattcagtattcag	59.6
3	283	gacagacaccaagaactgatgctgcctctg	aggggtgagggtcttgttagaagagggaaa	58.3
4	314	tcaccagtcatccctaggtccgtgcagcct	gagtgttgttccatgtgtctatgtctatgg	61.7
5	465	gcatctgctctgtaaagtgaa	gtccacctgtgctaggaatt	57.0, 61.4
6	256	caccctactgcggtct	agtcagggcaggtactttca	59.6, 61.5
7–9	736	gggcagttgggcagcta	acgtccccgtggagactttg	
7	180	cagctctgcctggtaaccattg	cttctgggcaaagactcaggc	60.7
8	262	gacaagccctgcactttcacc	gaaggcagggaaccccatc	61.2, 63.2
9	204	ccttgctggtgttcaggatg	gtggagactttgggtgagagg	61.4, 63.3
10, 11	390	accccatgcaaatgatcggtcttctctctc	gaccagagacttccctcatttctctattcc	60.0
12	283	cacgtctcaattcattgtctccg	acaggcaggagataggagt	61.7

rified PCR samples (5 μL) were separated on a heated C18 reverse phase column (DNASep) using 0.1 M triethylammonium acetate (TEAA) in water (Solvent A) and 0.1 M TEAA in 25% acetonitrile (Solvent B) at a flow rate of 0.9 mL/min. The software provided with the instrument selected the temperature for heteroduplex separation in the heterozygous *CYP4A22* fragments. Table 1 summarizes the DHPLC running conditions for each amplicon. The linear acetonitrile gradient was adjusted to the retention time of the DNA peak at 4–5 min.

Homozygous nucleotide exchanges can occasionally be distinguished because of a slight shift in the elution time as compared with the reference. The addition of an approximately equal amount of wild-type DNA to the samples (1:1) before the denaturation step enabled the reliable detection of homozygous alterations. This was performed routinely for all samples to identify homozygous sequence variations. Therefore, all samples were analyzed as follows: first, without mixing with an equal amount of wild-type DNA to detect heterozygotes, and then, after mixing each sample with wild-type DNA to detect homozygous variants. The resultant chromatograms were compared with those of the wild-type DNA.

2.4. Direct sequencing

Both strands of samples with variants as determined by DHPLC were analyzed using a CEQ8000 automated DNA sequencer (Beckman-Coulter Inc., Fullerton, CA, USA). We also sequenced all samples with chromatographic findings that differed from the wild type to establish links between mutations and specific profiles. We sequenced the PCR products by the fluorescent dideoxy termination using a DTCS DNA Sequencing Kit (Beckman-Coulter Inc.) in accordance with the manufacturer's instructions.

2.5. Haplotype analysis by cloning

In order to determine the linkage among these polymorphisms identified in this study, PCR reactions were used to amplify long fragments that were obtained from the individuals who were heterozygous for both the single nucleotide polymorphisms (SNPs). The fragment was run on a gel, the gel purified, and ligated to a pCR-2.1-TOPO vector or a pCR-XL-TOPO vector (Invitrogen Co., CA, USA). The ligation reaction was transfected into *Escherichia coli* strain TOP10 (Invitrogen Co., CA, USA), and single colonies (each containing a plasmid with only one of the two alleles) were grown and subjected to plasmid isolation and sequencing by using a CEQ8000 automated DNA sequencer.

3. Results

3.1. DHPLC and sequence analysis

The DHPLC analysis of the *CYP4A22* gene (12 exons) in 191 DNA samples obtained from Japanese individuals revealed chromatographic profiles that were distinct from the wild type in exons 1, 3–10, and 12. Representative DHPLC elution profiles are shown in Fig. 1. Direct sequencing analysis of the deviant DNAs detected by DHPLC revealed a total of 13 different polymorphisms in the exons (11 nonsynonymous and 2 synonymous SNPs). The locations and frequencies of these polymorphisms are described in Table 2. Among the polymorphisms identified in *CYP4A22*, two of these sequence variations correspond to silent mutations located in exons 8 (His323His) and 9 (Gly390Gly). Nine of these sequence variations correspond to missense mutations located in exons 1 (Arg11Cys), 3 (Arg126Trp), 4 (Gly130Ser and Asn152Tyr), 5 (Val185Phe), 6 (Cys231Arg), 7 (Lys276Thr), 10 (Leu428Pro), and 12 (Leu509Phe). One of these sequence variations corresponds to nonsense mutations located in exon 9 (Gln368stop). The 13th mutation corresponds to a nucleotide deletion (G9630del) that causes a frameshift and consequently results in a stop codon 80 nucleotides downstream. Exons 2 and 11 were devoid of polymorphic sites. Furthermore, we did not observe any variants affecting the exon–intron splice site recognition sequences, or any variants that would create new putative splice sites near the exon–intron boundaries.

Table 2
Frequencies of the human *CYP4A22* gene polymorphisms in 191 Japanese subjects

Locus	Position	Relative to the translation initiation site	Amino acid change	Frequency in Japanese subjects ($n = 191$)
343	Exon 1	31C>T	Arg11Cys	0.050
4436	Exon 3	4124C>T	Arg126Trp	0.555
4940	Exon 4	4628G>A	Gly130Ser	0.529
5006	Exon 4	4694A>T	Asn152Tyr	0.997
6138	Exon 5	5826G>T	Val185Phe	0.526
6644	Exon 6	6332T>C	Cys231Arg	0.974
7220	Exon 7	6908A>C	Lys276Thr	0.257
7379	Exon 8	7067G del		0.055
7448	Exon 8	7136C>T	His323His	0.380
7677	Exon 9	7365C>T	Gln368stop	0.003
7745	Exon 9	7433A>C	Gly390Gly	0.223
8753	Exon 10	8441T>C	Leu428Pro	0.552
11589	Exon 12	11277C>T	Leu509Phe	0.298

3.2. Haplotype analysis

Based on the concomitant occurrence of the polymorphisms among the individuals studied and the link-

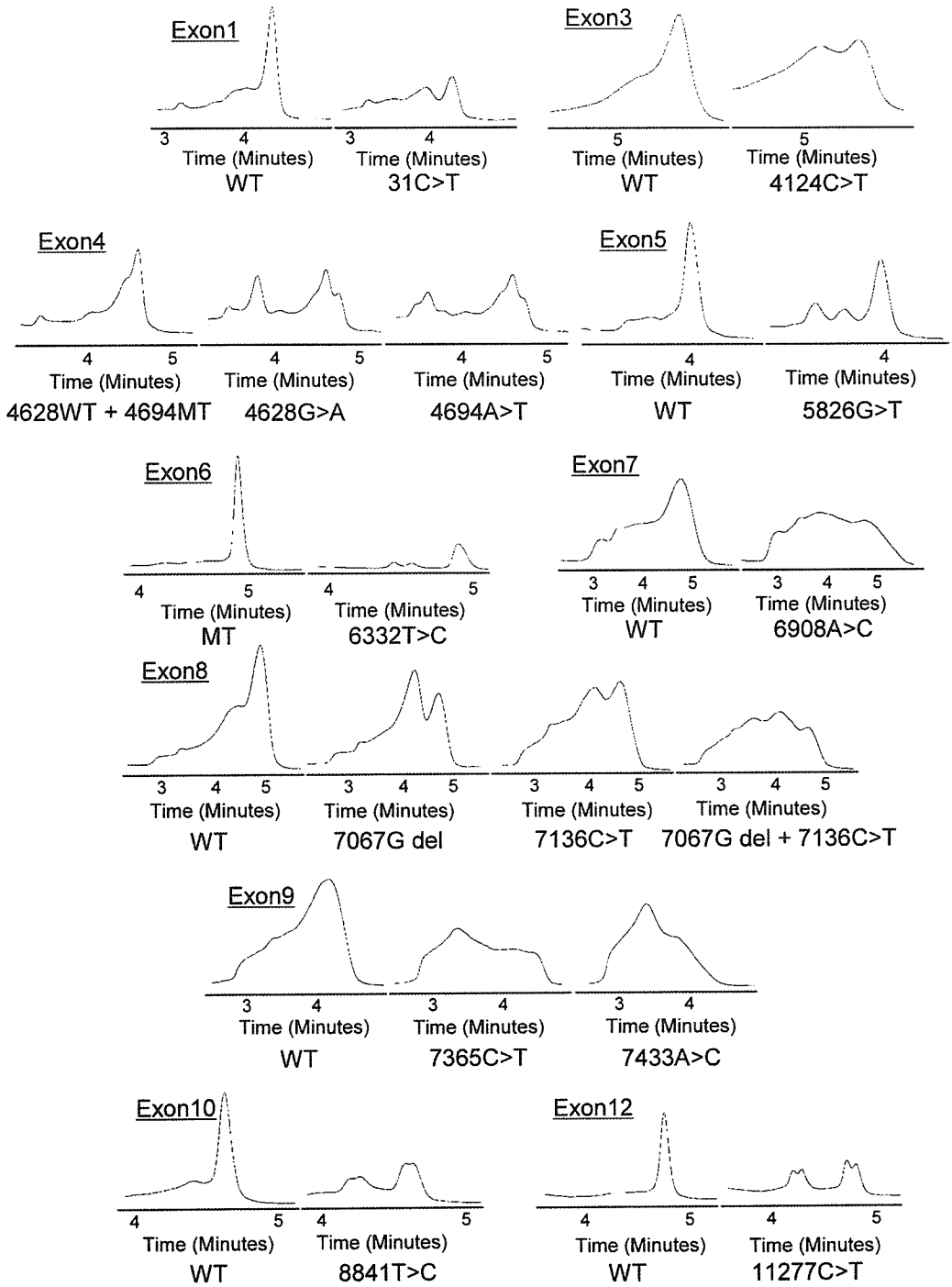

Fig. 1. DHPLC elution profiles that were previously within the coding region. WT, wild-type homozygote. MT, mutant-type homozygote.

age analysis by cloning, the different SNPs can be deduced to comprise 21 haplotypes, as described in Fig. 2. A genomic reference sequence with the accession number NT032977.7 was defined as the wild-type allele *CYP4A22*1*. The other alleles were named according to the recommendations of the CYP allele nomenclature committee (http://www.imm.ki.se/CYPalleles/). These allelic variants (*CYP4A22*2–*15*) discovered in this study have been submitted to the CYP alleles web page.

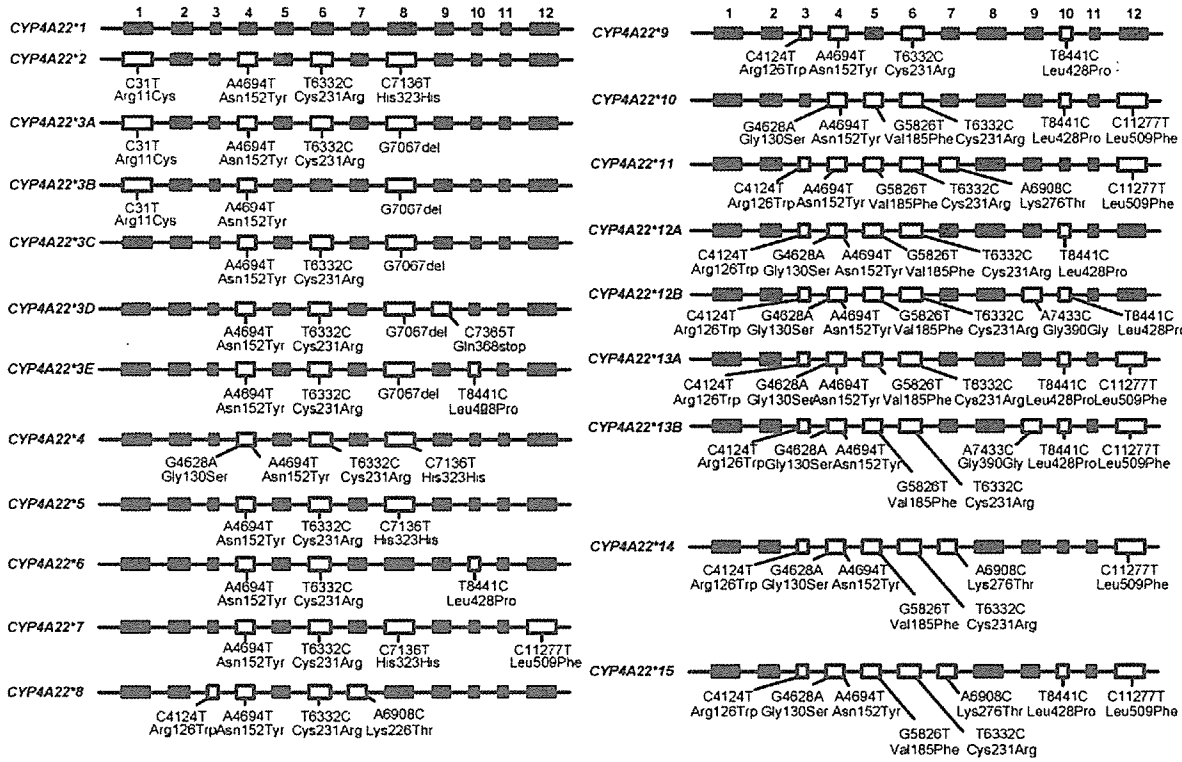

Fig. 2. Allelic variants of the human *CYP4A22* gene. Schematic representation of "wild-type" allele for *CYP4A22* (*CYP4A22*1*) and 20 variant alleles. The numbering is based on the first nucleotide of the initiation codon that is represented as 1. *CYP4A22** alleles were named in accordance with the established nomenclature for the *P450* alleles (http://www.imm.ki.se/CYPalleles/).

Table 3
Frequencies of the human *CYP4A22* alleles in 191 Japanese subjects

Allele	*n*	%	95% CI
**1*	1	0.26	0.00–0.77
**2*	1	0.26	0.00–0.77
**3A*	9	2.36	0.84–3.88
**3B*	9	2.36	0.84–3.88
**3C*	1	0.26	0.00–0.77
**3D*	1	0.26	0.00–0.77
**3E*	1	0.26	0.00–0.77
**4*	4	1.05	0.03–2.07
**5*	139	36.39	31.56–41.21
**6*	1	0.26	0.00–0.77
**7*	1	0.26	0.00–0.77
**8*	1	0.26	0.00–0.77
**9*	12	3.14	1.39–4.89
**10*	2	0.52	0.00–1.25
**11*	3	0.79	0.00–1.67
**12A*	5	1.31	0.17–2.45
**12B*	83	21.73	17.59–25.86
**13A*	8	2.09	0.66–3.53
**13B*	4	1.05	0.03–2.07
**14*	2	0.52	0.00–1.25
**15*	94	24.61	20.29–28.93
Total	382	100	

3.3. Allele and genotype frequencies

The frequencies of the alleles and genotypes discovered are listed in Tables 3 and 4, respectively. *CYP4A22*5* was the most common of the alleles. It occurred at a frequency of 36.39% in our study population (Table 3). The frequencies of the various genotypes observed in our Japanese study population followed those predicted by the Hardy–Weinberg law (Table 4). With the exception of the *CYP4A22*3B/*12B* genotype, these results were in good agreement with the expected genotype distributions that were calculated using the Hardy–Weinberg equation.

4. Discussion

In this study, we performed a comprehensive investigation of genetic variation in *CYP4A22*. In order to screen for sequence variations in the coding region of this gene, we developed a PCR-DHPLC assay that allows the molecular analysis of each exon of the gene. This is the first study to characterize the *CYP4A22* alleles and name them according to the recommended CYP allele nomenclature. Nine of the 13 SNPs detected in *CYP4A22* result

Table 4
Distributions of the human *CYP4A22* genotypes in 191 Japanese subjects

CYP4A22 genotype	Observed			Expected (%)
	n	%	95% CI	
**1/*15*	1	0.52	0.00–1.55	0.13
**2/*5*	1	0.52	0.00–1.55	0.19
**3A/*5*	8	4.19	1.35–7.03	1.72
**3A/*12B*	1	0.52	0.00–1.55	1.03
**3B/*12B*	9	4.71	1.71–7.72	1.03
**3C/*8*	1	0.52	0.00–1.55	0.001
**3D/*5*	1	0.52	0.00–1.55	0.19
**3E/*15*	1	0.52	0.00–1.55	0.13
**4/*11*	3	1.57	0.00–3.33	0.02
**4/*12B*	1	0.52	0.00–1.55	0.46
**5/*5*	26	13.61	8.75–18.48	13.24
**5/*9*	5	2.62	0.35–4.88	2.29
**5/*12A*	1	0.52	0.00–1.55	0.95
**5/*12B*	26	13.61	8.75–18.48	15.82
**5/*13A*	8	4.19	1.35–7.03	1.52
**5/*13B*	1	0.52	0.00–1.55	0.76
**5/*15*	36	18.85	13.30–24.40	17.91
**6/*14*	1	0.52	0.00–1.55	0.003
**7/*15*	1	0.52	0.00–1.55	0.130
**9/*12A*	1	0.52	0.00–1.55	0.08
**9/*12B*	2	1.05	0.00–2.49	1.36
**9/*15*	4	2.09	0.06–4.13	1.55
**10/*10*	1	0.52	0.00–1.55	0.003
**12A/*12B*	2	1.05	0.00–2.49	0.57
**12A/*15*	1	0.52	0.00–1.55	0.64
**12B/*12B*	10	5.24	2.08–8.40	4.72
**12B/*13B*	1	0.52	0.00–1.55	0.46
**12B/*15*	21	10.99	6.56–15.43	10.70
**13B/*13B*	1	0.52	0.00–1.55	0.01
**14/*15*	1	0.52	0.00–1.55	0.26
**15/*15*	14	7.33	3.63–11.03	6.06
Total	191	100.0		

in amino acid substitution. The alleles carrying these alterations were named *CYP4A22*2–*15*.

The rapid and high-throughput discovery of SNPs in genes associated with drug metabolism such as CYP enzymes is of increasing interest to pharmacogeneticists. Various methods have been developed to detect SNPs. Compared with single-strand conformation polymorphism analysis and other methods, DHPLC presents the advantages of high sensitivity, speed, and automation in searching for unknown SNPs. The procedure detects both missense and nonsense mutations. Sequencing offers the highest reliability for SNP discovery but the procedure is time-consuming and expensive. The cost of DHPLC is at least eight-fold lower than that for sequencing. The technology is well suited to detecting unknown SNPs in the genes for other drug metabolizing enzymes [12–14]. Based on DHPLC analysis of the PCR products, we developed a simple, rapid, and efficient strategy to analyze the *CYP4A22* gene sequence. This method involves the specific amplification of the 12 exons of the gene. The PCR-DHPLC procedure was applied to genomic DNA obtained from 191 individuals of Japanese origin. Under optimal experimental conditions, we observed clear differences in the elution profiles when a PCR product contained a variant allele. However, despite taking many precautions, some polymorphisms might have not been detected under these conditions.

Our investigation has enabled the identification of 13 mutations present in the *CYP4A22* coding region, demonstrating for the first time that this gene is subject to polymorphism. In particular, the variant corresponds to a nucleotide deletion (G7067del) that causes a frameshift and consequently results in a stop codon 80 nucleotides downstream. This mutation is likely to be responsible for the synthesis of a truncated protein that is 140 amino acids shorter than the wild-type protein. We can assume that at least the allele carrying G7067del encodes an inactive protein and contributes to the interindividual variability of the CYP4A22 enzymatic activity.

In this study, the sequence designated in NCBI as a genome reference sequence with the accession number NT032977.7 was defined as the wild-type allele *CYP4A22*1*. However, the allele has been detected in only one sample of Japanese subjects used in this study. The *CYP4A22*1* allele is very rare in the Japanese population. In contrast, the most common allele was *CYP4A22*5*. It occurred at a frequency of 36.39% in our study population. Further studies are required to confirm the structures of haplotypes in other populations.

The CYP4A22 cDNA was initially cloned from the human BAC library by Kawashima et al. [9] The *CYP4A22* and *CYP4A11* genes shared 95% sequence identity and have similar intron/exon sizes and distribution. However, the CYP4A22 mRNA is expressed at significantly lower levels than the CYP4A11 mRNA in the human liver and kidney samples [10]. Furthermore, Gainer et al. [8] found that *CYP4A22* that can only be detected at the mRNA level does not encode a functional protein; this is because of the substitution of the glycine at position 130, which is conserved among all CYP4A isoforms, by serine. In this study, we found several alleles carrying the serine at position 130 in the *CYP4A22* alleles (*CYP4A22*4*, **10*, **12A*, **12B*, **13A*, **13B*, **14*, and **15*). The enzyme proteins that were generated from these alleles might not have the catalytic activity toward arachidonic acid. Further studies are required to confirm the function of the CYP4A22 variant enzymes.

Recent studies have shown that CYP4A subfamilies metabolize endogenous compounds, such as arachidonic

acid and that these metabolites are associated with hypertension, thereby indicating interesting biological functions for these enzymes [15–17]. It has been reported that a coding variant (8590T > C) of the human *CYP4A11* gene that results in a CYP4A11 protein with reduced enzymatic activity has a greater prevalence in hypertensive Caucasians than in normotensive Caucasians [8]. If human *CYP4A22* is also involved in the metabolism of arachidonic acid, the sequence variation that we identified in the *CYP4A22* gene might have a significant impact on the regulation of blood pressure.

In summary, this comprehensive investigation of polymorphisms of the coding region of the *CYP4A22* gene identified 20 variant *CYP4A22* alleles (*CYP4A22*2–*15*). In vitro analysis of recombinant mutated cDNAs, as well as phenotyping studies, will help in determining the functions of the variants identified.

Acknowledgment

This work was supported in part by High-Tech Research Center Program of the Ministry of Education, Culture, Sports, Science, and Technology of Japan.

References

[1] R.T. Okita, J.R. Okita, Cytochrome P450 4A fatty acid omega hydroxylases, Curr. Drug Metab. 2 (2001) 265–281.
[2] S. Imaoka, H. Ogawa, S. Kimura, F.J. Gonzalez, Complete cDNA sequence and cDNA-directed expression of CYP4A11, a fatty acid omega-hydroxylase expressed in human kidney, DNA Cell. Biol. 12 (1993) 893–899.
[3] U. Hoch, Z. Zhang, D.L. Kroetz, P.R. Ortiz de Montellano, Structural determination of the substrate specificities and regioselectivities of the rat and human fatty acid omega-hydroxylases, Arch. Biochem. Biophys. 373 (2000) 63–71.
[4] J.H. Capdevila, J.R. Falck, The CYP P450 arachidonic acid monooxygenases: from cell signaling to blood pressure regulation, Biochem. Biophys. Res. Commun. 285 (2001) 571–576.
[5] J.C. McGiff, J. Quilley, 20-Hydroxyeicosatetraenoic acid and epoxyeicosatrienoic acids and blood pressure, Curr. Opin. Nephrol. Hypertens. 10 (2001) 231–237.
[6] R.J. Roman, P-450 metabolites of arachidonic acid in the control of cardiovascular function, Physiol. Rev. 82 (2002) 131–185.
[7] M. Ingelman-Sundberg, Human drug metabolising cytochrome P450 enzymes: properties and polymorphisms, Naunyn. Schmiedebergs. Arch. Pharmacol. 369 (2004) 89–104.
[8] J.V. Gainer, A. Bellamine, E.P. Dawson, K.E. Womble, S.W. Grant, Y. Wang, L.A. Cupples, C.Y. Guo, S. Demissie, C.J. O'Donnell, N.J. Brown, M.R. Waterman, J.H. Capdevila, Functional variant of CYP4A11 20-hydroxyeicosatetraenoic acid synthase is associated with essential hypertension, Circulation 111 (2005) 63–69.
[9] H. Kawashima, T. Naganuma, E. Kusunose, T. Kono, R. Yasumoto, K. Sugimura, T. Kishimoto, Human fatty acid omega-hydroxylase, CYP4A11: determination of complete genomic sequence and characterization of purified recombinant protein, Arch. Biochem. Biophys. 378 (2000) 333–339.
[10] U. Savas, M.H. Hsu, E.F. Johnson, Differential regulation of human CYP4A genes by peroxisome proliferators and dexamethasone, Arch. Biochem. Biophys. 409 (2003) 212–220.
[11] A. Bellamine, Y. Wang, M.R. Waterman, J.V. Gainer 3rd, E.P. Dawson, N.J. Brown, J.H. Capdevila, Characterization of the CYP4A11 gene, a second CYP4A gene in humans, Arch. Biochem. Biophys. 409 (2003) 221–227.
[12] M. Hiratsuka, H. Nozawa, Y. Konno, T. Saito, S. Konno, M. Mizugaki, Human CYP4B1 gene in the japanese population analyzed by denaturing HPLC, Drug Metab. Pharmacokinet. 19 (2004) 114–119.
[13] A. Ebisawa, M. Hiratsuka, K. Sakuyama, Y. Konno, T. Sasaki, M. Mizugaki, Two novel single nucleotide polymorphisms (SNPs) of the CYP2D6 gene in Japanese individuals, Drug Metab. Pharmacokinet. 20 (2005) 294–299.
[14] M. Hiratsuka, M. Kudo, N. Koseki, S. Ujiie, M. Sugawara, R. Suzuki, T. Sasaki, Y. Konno, M. Mizugaki, A novel single nucleotide polymorphism of the human methylenetetrahydrofolate reductase gene in Japanese individuals, Drug Metab. Pharmacokinet. 20 (2005) 387–390.
[15] C.L. Laffer, M. Laniado-Schwartzman, M.H. Wang, A. Nasjletti, F. Elijovich, Differential regulation of natriuresis by 20-hydroxyeicosatetraenoic acid in human salt-sensitive versus salt-resistant hypertension, Circulation 107 (2003) 574–578.
[16] C.L. Laffer, M. Laniado-Schwartzman, M.H. Wang, A. Nasjletti, F. Elijovich, 20-HETE and furosemide-induced natriuresis in salt-sensitive essential hypertension, Hypertension 41 (2003) 703–708.
[17] I. Fleming, Cytochrome P-450 under pressure: more evidence for a link between 20-hydroxyeicosatetraenoic acid and hypertension, Circulation 111 (2005) 5–7.

Progressive Vacuolating Glycine Leukoencephalopathy with Pulmonary Hypertension

Mireia del Toro, MD,[1] José Antonio Arranz, MS,[2] Alfons Macaya, MD, PhD,[1] Encarnació Riudor, MS,[2] Miquel Raspall, MD,[1] Antonio Moreno, MD,[3] Elida Vazquez, MD,[4] Arancha Ortega, MD,[5] Yoichi Matsubara, MD,[6] Shigeo Kure, MD,[6] and Manuel Roig, MD, PhD[1]

To report two unrelated patients with a new phenotype of nonketotic hyperglycinemia associated with idiopathic pulmonary hypertension. Clinical findings included rapidly progressive neurological deterioration with onset in the first year of life characterized by developmental regression without seizures or electroencephalogram abnormalities during follow-up. Both patients died before the age of 18 months. Glycine cleavage system deficiency was confirmed by enzymatic studies in frozen liver. Molecular analysis in the related genes showed no pathogenic mutation. Radiological and pathological findings were consistent with progressive vacuolating encephalopathy. Our patients with biochemical and enzymatic parameters consistent with atypical nonketotic hyperglycinemia. The clinical and radiological evolution, as progressive vacuolating leukoencephalopathy and the association with pulmonary hypertension constitute a previously unrecognized variant.

Ann Neurol 2006;60:148–152

Nonketotic hyperglycinemia (NKH; OMIM 238300) is an autosomal recessive inborn error of glycine metabolism. The most frequent and severe presentation is the classic or neonatal form. Atypical forms include infantile NKH, mild episodic NKH, late-onset NKH, and transient NKH. The primary metabolic defect involves the glycine cleavage system (GCS), an intramitochondrial complex with four subunits.[1,2] Defects in the protein P subunit account for 80% of neonatal NKH cases. The gene encoding human P protein has been located in chromosome 9.[3]

Idiopathic pulmonary hypertension (IPH) is a rare disorder with an incidence of one to two cases per million individuals per year. A positive family history is reported in at least 6% of patients. Familial cases are inherited as an autosomal dominant disorder with reduced penetrance and genetic anticipation. The gene for IPH, bone morphogenetic protein receptor II *(BMPR2)*, is located in chromosome 2 and is a member of the transforming growth factor-β superfamily of receptors.[4]

In 1992, we reported three siblings with an atypical form of NKH presenting in the first months of life with progressive neurological deterioration associated with pulmonary hypertension and hyperglycinemia in plasma, urine, and cerebrospinal (CSF), with a plasma/CSF ratio in the range of atypical NKH.[5] Brain magnetic resonance imaging (MRI) and autopsy were not performed in these patients. We recently identified two new unrelated patients with this same clinical association and reported their biochemical findings.[6] The clinical, neuroradiological, and pathological findings of these two patients are described herein.

Case Reports

Patient 1

The patient was the first son of healthy nonconsanguineous parents, born of an uneventful pregnancy and delivery. At 2 months old, he was diagnosed with IPH (pulmonary artery pressures measured at catheterization: 40/10–25mm Hg). Reportedly, psychomotor development was normal until the age of 8 months when neurological deterioration developed 1 week after immunization (DTP+Hib+polio+meningococcus). Physical examination showed an alert child with severe hypotonia and hypoactivity, hyperreflexia, Achilles clonus, and bilateral Babinski sign. He suffered tonic spasms with opisthotonic posturing during which consciousness was preserved.

Electroencephalogram (EEG) was normal. Brain MRI (Figs 1A, B) showed bilateral confluent areas of abnormal signal intensity involving occipital white matter. Metabolic studies were consistent with atypical NKH: high plasma glycine (768μmol/L; reference range, 125–318), high CSF glycine (45μmol/L; reference range, 3.8–7.9), and high CSF/plasma glycine (ratio, 0.059; reference range, 0.012–0.040). Organic acidurias were ruled out by complete urine studies. Lactate levels in plasma and CSF were also normal.

Neurological deterioration progressed to an abnormal breathing pattern with polypnea and apneic spells, severe hypotonia, and frequent opisthotonic spasms. A second MRI at the age of 12 months (see Figs 1C–F) showed signs of progression with cysts in temporal lobes. Magnetic resonance spectroscopy (MRS) showed

From the [1]Secció de Neurologia Infantil, [2]Laboratori de Malalties Metabòliques, [3]Secció de Pneumologia Infantil, [4]Institut de Diagnòstic per la Imatge, and [5]Servei d'Anatomia Patològica, Hospital Universitari Vall d'Hebron, Barcelona, Spain; and [6]Department of Medical Genetics, Tohoku University School of Medicine, Sendai, Japan.

Received Jan 5, 2006. Accepted for publication Apr 15, 2006.

Published online June 26, 2006 in Wiley InterScience (www.interscience.wiley.com). DOI: 10.1002/ana.20887

Address correspondence to Dr Roig, Pediatric Neurology Unit, Hospital Vall d'Hebron, Passeig Vall d'Hebron 119-129, 08035 Barcelona, Spain. E-mail: manroig@cs.vhebron.es

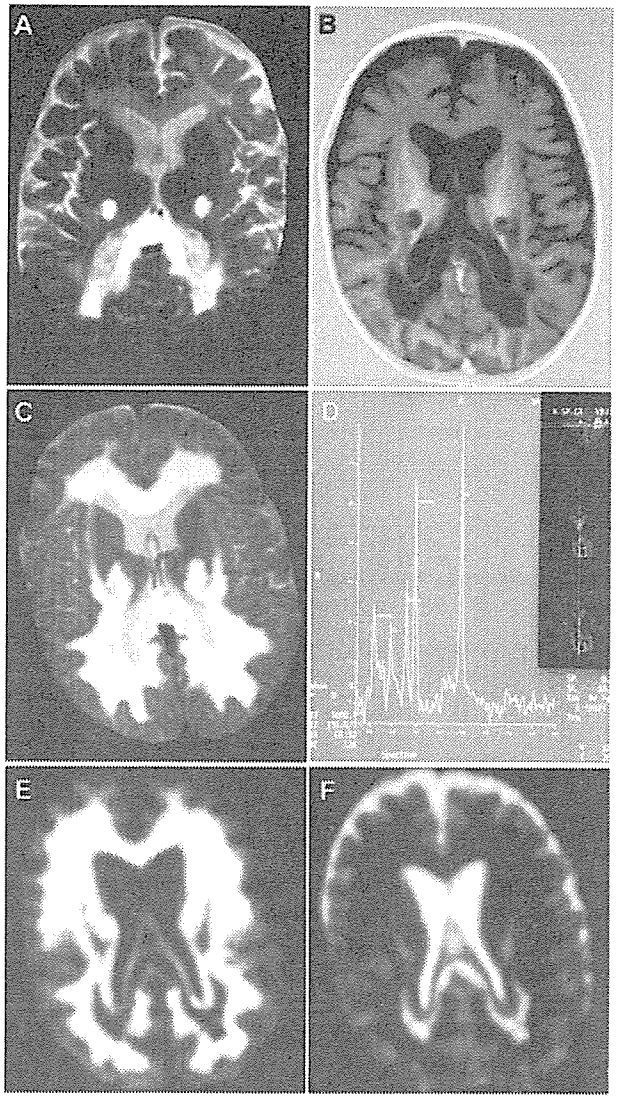

Fig 1. First magnetic resonance images (A, B) show bilateral abnormal signal intensity areas on T1 and T2, involving occipital white matter, corpus callosum, and both internal capsulae. Lesions are symmetric and confluent, without contrast enhancement, and spare subcortical U-fibers. Second magnetic resonance images shows progression with bilateral extensive lesions on axial T2-weighted imaging, involving external capsulae and frontal white matter (C). Magnetic resonance spectroscopy in long echo time spectrum shows an abnormal glycine peak at 3.56 (D). Peripheral restricted diffusion coefficient on diffusion imaging. (E) and apparent diffusion coefficient (F) maps suggests acute myelin vacuolation, with a central hypointense necrotic area.

a glycine peak at 3.56 parts per million. Respiratory complications led to death of the patient at the age of 14 months.

Enzyme studies in a liver specimen obtained and frozen immediately after death showed low activity of the GCS (0.34nkat/kg protein; reference range, 110 ± 41nkat/kg protein) and undetectable activity of the P protein of the complex (performed by Dr O. Rolland, Hôpital Debrousse, Lyon, France). Other liver enzyme activities studied at the same time were normal. Screening for mutations in entire coding regions of the *GLDC* (protein P), *AMT* (protein T), and *GCSH* (protein H) genes was performed as described elsewhere.[7] One heterozygous base change, c.2852C>A, was found in *GLDC* exon 24, which caused amino acid substitution from 951Ser to 951Tyr (S951Y). Expression analysis in COS7 cells showed that *GLDC* complementary DNA with the S951Y mutation had 39% enzymatic residual activity compared with normal complementary DNA.

Macroscopic examination of the brain (Fig 2) showed symmetric involvement with softening and swelling of white matter and cavitated areas in temporooccipital lobes. Microscopic studies detected loss of myelin with spongiform degeneration and vacuolation, decreased oligodendrocyte density, reactive astrogliosis, and macrophagic infiltration. Corpus callosum, cerebellar white matter, and pyramidal tracts were involved. U-fibers were partially preserved.

Patient 2

The patient was the first daughter of healthy nonconsanguineous parents, born of an uneventful pregnancy and delivery. Her initial psychomotor development was normal. At the age of 8 months, she was diagnosed with IPH (pulmonary artery pressures: 57/19–34mm Hg). At 11 months old, during a febrile episode, she suffered acute neurological deterioration with hypotonia and hypoactivity. She was referred to our hospital 1 month later. Neurological examination showed an alert girl, with poor social interaction, mild hypotonia, bilateral hyperreflexia, Achilles clonus, and bilateral Babinski sign.

EEG was normal. Brain MRI (Fig 3) showed diffuse white matter involvement with increased high-signal intensity on T2-weighted images affecting periventricular areas and occipital lobes, preserving subcortical U-fibers. Glycine levels in plasma and CSF were high (950 and 37μmol/L, respectively) with a CSF/plasma ratio of 0.039, consistent with atypical NKH. Her neurological status deteriorated with progressive hypoactivity and episodes of rigid spasms and opisthotonic posturing. She died at the age of 13 months.

Enzyme studies in frozen liver showed undetectable activity of both the GCS and P protein (Dr O. Roland). Control liver enzyme activities, run concurrently, were normal. Analyses of the complete coding sequence and intronic flanks were also performed in the *GLDC*, *AMT*, and *GCSH* genes as described elsewhere,[7] but failed to detect any alteration. Normal chorionic villi GCS activity was used successfully for genetic counseling in a further pregnancy.

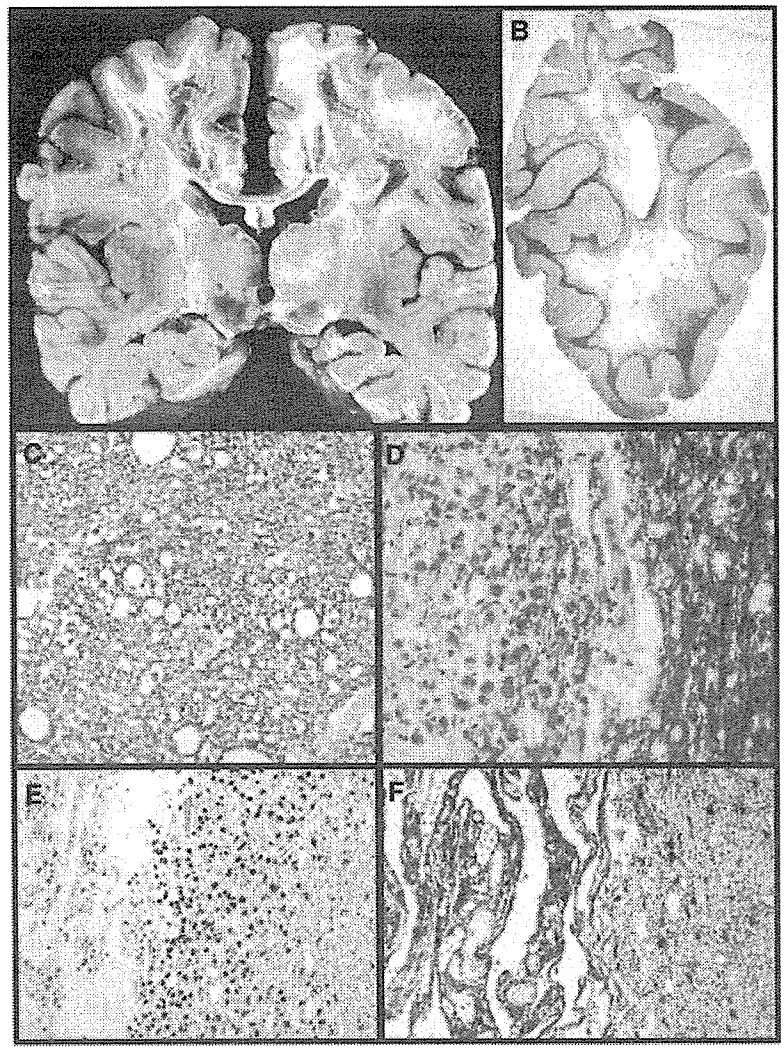

Fig 2. (A) Extensive bilateral cavitation of white matter with corpus callosum involvement in coronal section. (B) Myelin-stained occipital lobe with extensive demyelination and spared arcuate fibers. (C) Spongy degeneration; diffuse white matter vacuolar changes are evident in cerebellum, brainstem, and pons (Luxol fast blue/cresyl violet). Original magnification ×100. (D) Demyelinating process in a cavitated area with isolated myelin fragments, dense macrophagic infiltration, and absence of oligodendrocytes in the left side. In the right side, white matter is preserved (Luxol fast blue/cresyl violet). Original magnification ×100). (E) Microglial activation and macrophagic infiltration shows intense cytoplasmic immunoreactivity for CD68 antibody in the periphery of cavitated areas. Original magnification ×40. (F) In contrast, intense astrogliosis is evident with glial fibrillary acidic protein antibody in cavitated areas, whereas peripheric astrocytosis is mild. Original magnification ×40.

Results and Discussion

The main clinical features of these patients, and those reported in 1992, included onset in infancy of IPH and rapidly progressive encephalopathy, leading to death before the age of 18 months. All the patients showed hypotonia, pyramidal signs, and respiratory abnormalities. No seizures or paroxysmal EEG abnormalities were found. Neuroimaging demonstrated severe symmetrical cystic leukoencephalopathy affecting particularly temporooccipital lobes. Pathology studies in Patient 1 showed diffuse white matter spongiform degeneration, decreased oligodendrocyte density, reactive astrogliosis, and macrophagic infiltration. Biochemical studies were consistent with atypical NKH.[8]

Patients with the infantile NKH phenotype usually present with seizures and psychomotor regression of variable severity after 6 months of age, and unlike neonatal patients, they have long survival without respiratory disorders.[9–11] CSF/plasma glycine ratios are usually above 0.09 in typical (neonatal) NKH and may vary from 0.04 to 0.10 in atypical cases. Our patients differed from this pattern in the absence of seizures or paroxysmal EEG abnormalities and the presence of a significant respiratory disturbance pattern. However,

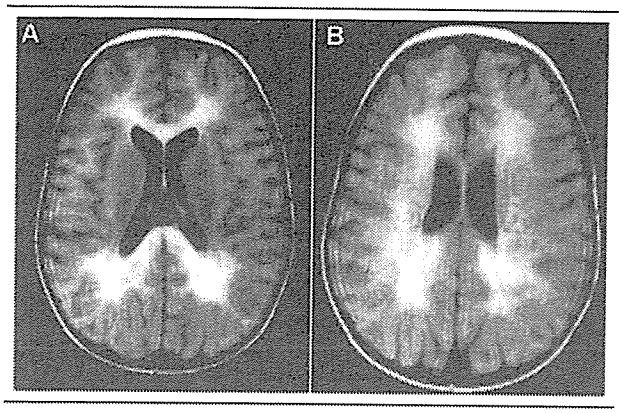

Fig 3. (A, B) Abnormal signal intensity on fluid-attenuated inversion recovery images involving frontal and occipital periventricular white matter. Lesions extend across midline involving splenium of corpus callosum, with subcortical U-fiber preservation.

the finding of decreased activity in GCS with undetectable P protein activity and normal activities of all other enzymes tested confirmed the diagnosis of NKH. The absence of mutations in the known GCS protein genes suggests the possibility of participation of other genes.

Neuropathological findings in Patient 1 were similar to those described in classic NKH: spongiform degeneration of white matter affecting cerebral lobes, cerebellum, and brainstem. On microscopic examination, studies of involved areas of centrum semiovale and parietooccipital lobes showed cavitation with preserved arcuate fibers, loss of myelinated axons, and massive absence of oligodendrocytes. The corpus callosum, as well as pyramidal tracts, was also involved. The myelin defect could be partially explained by a deficient synthesis due to lack of oligodendrocites.[12,13]

The association between NKH and pulmonary hypertension was described previously in four patients.[14] Two were older than our patients at diagnosis (3 and 6 years old) and presented with mild neurological symptoms. One of these patients had pulmonary hypertension as the predominant feature, which was the cause of death 1 year after diagnosis. The other two cases were diagnosed with neonatal NKH (with congruent clinical and EEG findings) at birth and later developed hypoxemia, which led to the diagnosis of IPH. The clinical course in all four cases was different from that of our patients. Although evidence exists of GCS messenger RNA expression in lungs (particularly H and T protein and, very weakly, P protein),[15] the pathophysiological relation between both entities remains unknown. We believe that pulmonary changes could be related to glycine toxicity or to a contiguous gene syndrome.

The clinical phenotype of our patients could resemble the severe variant form of childhood ataxia with central hypomyelination (CACH)/vanishing white matter (VWM) disease related to eIF21B subunit gene mutations.[16,17] Patients with VWM have shown raised CSF glycine. Although concentrations were not as high as those found in atypical NKH, the glycine CSF/plasma ratio was above normal values and reached the minimum value required as a criterion for NKH. The significance of this finding has not been established, but it could be related to excitotoxic brain damage.[18] Cystic white matter degeneration is characteristic of VWM both in classic and severe forms of the disease. In VWM, histopathological studies show myelin spongy and cystic degeneration. U-fibers and cortex usually are spared. The most characteristic finding is the presence of foamy oligodendrocytes with reduced astroglia, which differs from the findings in our patients.[19]

Glycine acts as an inhibitory neurotransmitter at specific brainstem and spinal cord receptors. Enhanced inhibitory activity leads to lethargy, hypotonia, pyramidal signs, and abnormalities in breathing patterns. Glycine also plays an excitatory neurotransmitter role in the central nervous system by acting at the modulatory site of the *N*-methyl-D-aspartate glutamate receptor.[2,20] This action may account for the intractable seizures in classic NKH. Therefore, we suspect that the symptoms in our patients may have been related to the increased inhibitory effect of glycine rather than to glycine-mediated excitotoxic brain injury.

In conclusion, our patients presented glycine encephalopathy with biochemical and enzymatic parameters consistent with atypical NKH. The clinical and radiological evolution, as progressive vacuolating leukoencephalopathy, absence of seizures, and association with pulmonary hypertension constitute, to our knowledge, a previously unrecognized variant.

This work was supported by REDEMETH (G03/54), M.d.T., J.A.A., E.R.

We are grateful to C. O'Hara for her assistance in the English version of the manuscript.

References

1. Tada K, Kure S. Nonketotic hyperglycinemia: molecular lesion, diagnosis and pathophysiology. J Inherit Metab Dis 1993;16: 691–703.
2. Hamosh A, Johnston M. Nonketotic hyperglycinemia. In: Scriver CR, Beaudet AL, Sly WS, Valle D, eds. The metabolic and molecular bases of inherited disease. Vol II. 8th ed. New York: McGraw-Hill, 2001:2065–2078.
3. Kure S, Kojima K, Ichinohe A, et al. A comprehensive mutation analysis of *GLDC*, *AMT* and *GCSH* in glycine encephalopathy. J Inherit Metab Dis 2003;26:66.
4. Deng Z, Morse JH, Slager SL et al. Familial primary pulmonary hypertension (gene PPH1) is caused by mutations in the bone morphogenetic protein receptor-II gene. Am J Hum Genet 2000;67:737–744.
5. Riudor E, Urgelles M, Colomer L, et al. Familial pulmonary hypertension with non ketotic hyperglycinemia (Abstract). Paper presented at: 30th SSIEM Conference; 1992; Leuven, Belguim; p. A38.

6. Riudor E, Arranz JA, del Toro M, et al. A new presentation of non ketotic hyperglycinemia with primary pulmonary hypertension and branched acylglycines with fatal outcome in three families. J Inherit Metab Dis 2001;24(suppl 1):35.
7. Kure S, Ichinohe A, Kojima K, et al. Mild variant of nonketotic hyperglycinemia with typical neonatal presentations: mutational and the in vitro expression analyses in two patients. J Pediatr 2004;144:827–829.
8. Applegarth DA, Toone JR. Nonketotic hyperglycinemia (glycine encephalopathy): laboratory diagnosis. Mol Genet Metab 2001;74:139–146.
9. Applegarth DA, Toone JR. Glycine encephalopathy (non ketotic hyperglycinemia): review and update. J Inherit Metab Dis 2004;27:417–422.
10. Holmgren G, Blomquist HK. Non ketotic hyperglycinemia in two sibs with mild psycho-neurological symptoms. Neuropediatrics 1977;8:67–72.
11. Trauner DA, Page T, Greco C, et al. Progressive neurodegenerative disorder in a patient with nonketotic hyperglycinemia. J Pediatr 1981;98:272–275.
12. Shuman RM, Leech RW, Scott RC. The neuropathology of the nonketotic and ketotic hyperglycinemias: three cases. Neurology 1978;28:139–146.
13. Agamanolis DP, Potter JL, Herrick MK, Sternberger NH. The neuropathology of glycine encephalopathy: a report of five cases with immunohistochemical and ultrastructural observations. Neurology 1982;32:975–985.
14. Cataltepe S, Van Marter LJ, Hozakewich H, et al. Pulmonary hypertension associated with nonketotic hyperglycinemia. J Inherit Metab Dis 2000;23:137–144.
15. Kure S, Kojima K, Kudo T, et al. Chromosomal localization, structure, single-nucleotide polymorphisms, and expression of the human H-protein gene of the glycine cleavage system (GCSH), a candidate gene for nonketotic hyperglycinemia. J Hum Genet 2001;46:378–384.
16. Fogli A, Dionisi-Vici C, Deodato F, et al. A severe variant of childhood ataxia with central nervous system hypomyelination/vanishing white matter leukoencephalopathy related to *EIF2B5* mutation. Neurology 2000;59:1966–1968.
17. Van der Knaap MS, van Berkel CG, Herms J, et al. eIF2B-related disorders: antenatal onset and involvement of multiple organs. Am J Hum Genet 2003;73:1199–1207.
18. Van der Knaap MS, Wevers RA, Kure S, et al. Increased cerebrospinal fluid glycine: a biochemical marker for a leukoencephalopathy with vanishing white matter. J Child Neurol 1999;14:728–731.
19. Rodriguez D, Gelot A, Della Gaspera B, et al. Increased density of oligodendrocytes in childhood ataxia with diffuse central hypomyelination (CACH) syndrome: neuropathological and biochemical studies of two cases. Acta Neuropathol 1999;97:469–480.
20. Ichinohe A, Kure S, Mikawa S, et al. Glycine cleavage system in neurogenic regions. Eur J Neurosci 2004;19:2365–2370.

13. Nishigaki Y, Marti RA, Hirano M. ND5 is a hotspot for multiple atypical mitochondrial DNA deletions in mitochondrial neurogastrointestinal encephalomyopathy. Hum Mol Genet 2004;13:91–101.
14. Filosto M, Mancuso M, Nishigaki Y, et al. Clinical and genetic heterogeneity in progressive external ophthalmoplegia due to mutations in polymerase γ. Arch Neurol 2003;60:1279–1284.
15. Tay SKH, Akman HO, Chung WK, et al. Fatal infantile neuromuscular presentation of glycogen storage disease type IV. Neuromusc Disord 2004;14:253–260.
16. Luoma PT, Luo N, Loscher WN, et al. Functional defects due to spacer-region mutations of human mitochondrial DNA polymerase in a family with an ataxia-myopathy syndrome. Hum Mol Genet 2005;14:1907–1920.
17. Shiba M, Bower JH, Maraganore DM, et al. Anxiety disorders and depressive disorders preceding Parkinson's disease: a case-control study. Movement Disord 2000;15:669–677.
18. De Coo IFM, Renier WO, Ruitenbeek W, et al. A 4-base pair deletion in the mitochondrial cytochrome *b* gene associated with Parkinsonism/MELAS overlap syndrome. Ann Neurol 1999;45:130–133.
19. Thyagarajan D, Bressman S, Bruno C, et al. A novel mitochondrial 12S rRNA point mutation in Parkinsonism, deafness and neuropathy. Ann Neurol 2000;48:730–736.
20. Mancuso M, Filosto M, Oh SJ, DiMauro S. A novel *POLG* mutation in a family with ophthalmoplegia, neuropathy, and parkinsonism. Arch Neurol 2004;61:1777–1779.

Rapid Diagnosis of Glycine Encephalopathy by ^{13}C-Glycine Breath Test

Shigeo Kure, MD,[1] Stanley H. Korman, MBBS, FRACP,[2] Junko Kanno, MD,[1] Ayumi Narisawa, MD,[1] Mitsuru Kubota, MD,[3] Toshimitsu Takayanagi, MD,[4] Masaki Takayanagi, MD,[5] Takashi Saito, MD,[6] Akira Matsui, MD,[6] Fumiaki Kamada, MD,[1,7] Yoko Aoki, MD,[1] Toshihiro Ohura, MD,[8] and Yoichi Matsubara, MD[1,7]

Objective: It is currently problematic to confirm the clinical diagnosis of glycine encephalopathy, requiring either invasive liver biopsy for enzymatic analysis of the glycine cleavage system or exhaustive mutation analysis. Because the glycine cleavage system breaks down glycine generating carbon dioxide, we suppose that the glycine cleavage system activity could be evaluated *in vivo* by measuring exhaled $^{13}CO_2$ after administration of [1-^{13}C]glycine.
Methods: The [1-^{13}C]glycine breath test was performed in 10 control subjects and 5 glycine encephalopathy patients with *GLDC* mutation, including 1 patient with mild glycine encephalopathy.
Results: All the patients showed lower $^{13}CO_2$ excretion than any control subject.
Interpretation: Not only typical GE but also atypical GE can be reliably diagnosed by the ^{13}C-glycine breath test. Because it is rapid, non-invasive, and requires little expertise, the breath test could be useful as a standard test for diagnosing GE.

Ann Neurol 2006;59:862–867

Glycine encephalopathy (GE; MIM 605899), also termed nonketotic hyperglycinemia (NKH), is an inborn error of glycine metabolism caused by deficiency

From the [1]Department of Medical Genetics, Tohoku University School of Medicine, Sendai, Japan; [2]Metabolic Diseases Unit, Division of Pediatrics, Hadassah-Hebrew University Medical Center, Jerusalem, Israel; [3]Department of Pediatrics, Hokkaido University Hospital, Sapporo; [4]Department of Pediatrics, National Organization Saga Hospital, Saga; [5]Department of Metabolic Disorder, Chiba Children's Hospital, Chiba; [6]Department of Pediatrics, Institute of Clinical Medicine, University of Tsukuba, Tsukuba; [7]Tohoku University 21st COE Program "Comprehensive Research and Education Center for Planning of Drug Development and Clinical Evaluation"; and [8]Department of Pediatrics, Tohoku University School of Medicine, Sendai, Japan.

Received Jan 14, 2006, and in revised form Feb 20. Accepted for publication Mar 10, 2006.

Published online Apr 24, 2006, in Wiley InterScience (www.interscience.wiley.com). DOI: 10.1002/ana.20853

Address correspondence to Dr Kure, Department of Medical Genetics, Tohoku University School of Medicine, 1-1 Seiryomachi, Aobaku, Sendai 980-8574, Japan. E-mail: skure@mail.tains.tohoku.ac.jp

of the glycine cleavage system (GCS). Classically, GE presents in the first days of life with progressive lethargy, hypotonia, and apnea, usually leading to coma and death unless assisted with ventilation.[1–3] Patients with atypical GE often lack neonatal symptoms, but present later with a variety of neurological symptoms including seizures, cognitive impairments, and abnormal behaviors.[4–7] Because these atypical patients manifest only nonspecific clinical symptoms, their diagnosis may be delayed or missed.

The biochemical hallmark of GE is an elevated ratio of the cerebrospinal fluid/plasma glycine concentration.[2,3] In atypical GE cases, there can be considerable residual GCS activities and the elevation of the ratio may be borderline or even absent. Furthermore, increased glycine levels and ratio also have been observed in other pathological conditions or with administration of certain drugs.[8] Therefore, the clinical diagnosis requires confirmation either by enzymatic analysis of the GCS in biopsies of liver specimens or by the exhaustive mutational analysis of three responsible genes, *GLDC, AMT,* and *GCSH.* Both procedures are laborious, require technical expertise, and currently are performed in only a few laboratories worldwide. It is therefore desirable to develop a rapid and simple diagnostic method that can be performed in hospitals and clinics.

We have developed a simple breath test for the enzymatic diagnosis of GE. When glycine is administered to healthy subjects, it should be decarboxylated predominantly by the GCS, leading to production of CO_2, as illustrated in Figure 1A.[9] The amount of CO_2 production may be quantified easily if glycine is labeled with stable isotope ^{13}C, which can be administered safely to patients.[10] To test the feasibility of the [1-^{13}C]glycine (^{13}C-glycine) breath test, we performed it in control subjects and GE patients in whom the diagnosis had been confirmed by the genetic test.

Subjects and Methods

Patients and Control Subjects

We performed the breath test in five patients (Patients 1–5) whose diagnosis of GE was confirmed by the mutational analysis of the *GLDC* gene. Mutational analysis of GE patients was performed by sequencing all the *GLDC* exons, as described previously.[11,12] Clinical features and the identified *GLDC* mutations are summarized in the Table. Patient 6 was given a diagnosis of vitamin B_{12} nonresponsive methylmalonic acidemia (MIM 251000) in infancy. He is now 7 years old and has been treated successfully by gastric infusion of special milk formula. The breath test also was performed in 10 healthy control subjects aged 16 to 45 years.

^{13}C-Glycine Breath Test

The breath test was performed in the outpatient setting. ^{13}C-glycine with more than 99% purity was purchased from Cambridge Isotope Laboratories (Andover, MA). A dose of 10mg/ml ^{13}C-glycine saline solution was sterilized with a

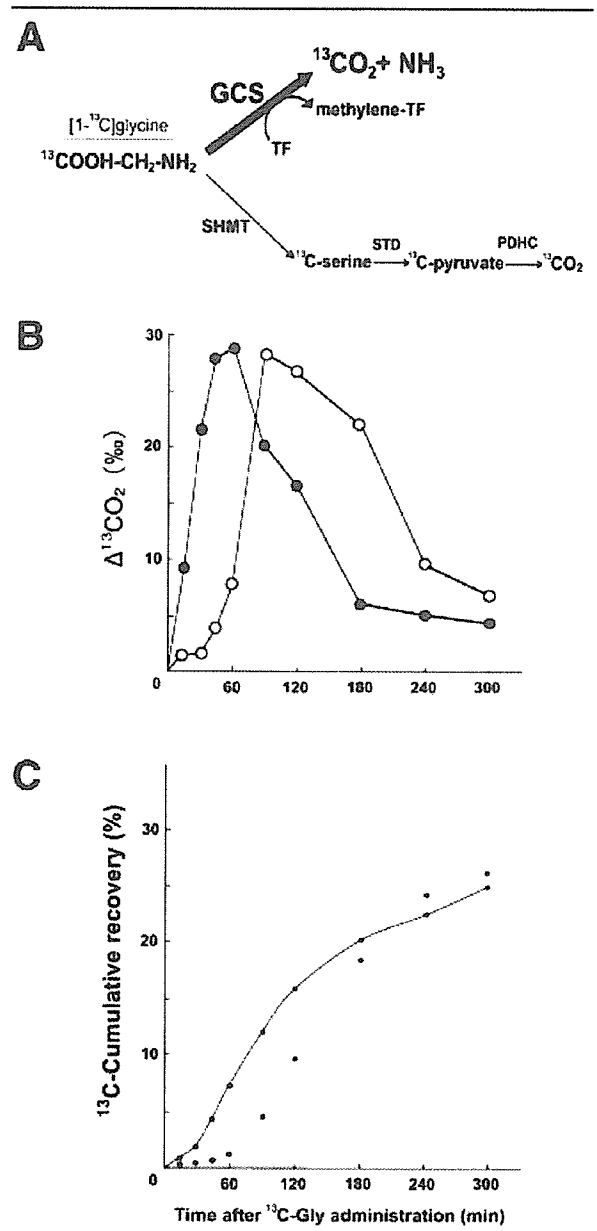

Fig 1. Breakdown of administered ^{13}C-glycine in vivo. Oxidation of ^{13}C-glycine by the glycine cleavage system (GCS) and the other metabolic pathway (A). Administered ^{13}C-glycine is degraded mainly by the GCS to generate $^{13}CO_2$, whereas a small part of the ^{13}C-glycine is degraded sequentially by serine hydroxymethyl transferase (SHMT), serine-threonine dehydratase (STD), and pyruvate dehydrogenase complex (PDHC), resulting in the production of $^{13}CO_2$. Results of two representative ^{13}C-glycine breath tests performed in the same control subject, indicating the time course of $\Delta^{13}CO_2$ excretion (B) and the ^{13}C-cumulative (%) recovery (C). Note that the ^{13}C-cumulative recoveries at 300 minutes are similar, whereas $\Delta^{13}CO_2$ excretion reached peak values at different time points.

Table. Profiles of Glycine Encephalopathy Patients

Characteristics	Patient No.				
	1	2	3	4	5
Sex	M	M	M	F	F
Ethnicity	Asian	Asian	Asian	Asian	Arab
Current age	2 yr 4 mo	6 yr 10 mo	1 yr 0 mo	11 yr 6 mo	12 yr 8 mo
Age of onset	3 days	2 days	1 day	1 day	2 days
Initial symptoms	Hypotonia, seizure	Coma, hypotonia	Hypotonia	Coma, hypotonia	Coma, hypotonia
Psychomotor development					
Head control	No	No	No	Yes	Yes
Sitting alone	No	No	No	Yes	Yes
Walking alone	No	No	No	Yes	Yes
Glycine concentration					
CSF glycine concentration (reference range: 2.9-10.4), μM	113	148	33	57	74
Plasma glycine concentration (reference range: 56-308), μM	500	1,220	193	659	585
CSF/serum glycine ratio (reference: <0.04), μM	0.22	0.12	0.17	0.09	0.13
GLDC mutation					
Allele 1	Y858X	N150T (1%)[a]	T269M	N150T (1%)[a]	A802V (32%)[a]
Allele 2	Large deletion	IVS7+1G>A	IVS2+1G>A	R790W (14%)[a]	A802V (32%)[a]
Age at breath test	1 yr 9 mo	5 yr 11 mo	1.5 mo	9 yr 3 mo	12 yr 0 mo
^{13}C-cumulative recovery in breath test (mean ± SD in control subjects: 24.1 ± 4.0%)	4.6%	7.9%	8.7%	9.3%	10.8%
Reference	This study	This study	This study	Kure and colleagues, 2004[12]	Korman and colleagues, 2004[18]

[a]Figures in parentheses indicate the residual glycine cleavage system activity estimated by the in vivo expression analysis in COS7 cells. CSF = cerebrospinal fluid; SD = standard deviation.

Millex-GV 0.22μm filter (Millipore, Billerica, MA) just before use. A dose of 10mg/kg of ^{13}C-glycine, up to a maximum dosage of 100mg, was administered through gastric tubes in Patients 1, 2, 3 and 6, whereas it was given orally to the control subjects and to Patients 4 and 5. Before the administration of ^{13}C-glycine, a 1,300ml reference breath sample was collected. The control subjects and Patients 5 and 6 breathed directly into the breath sampling bags (Otsuka Electronics, Osaka, Japan), whereas the breath samples for Patients 1 through 4 were collected using a face mask equipped with a one-way air valve (Vital Signs, Totowa, NJ), followed by transfer to the sampling bags. Test samples of 150 to 250ml were collected at 15, 30, 45, 60, 90, 120, 180, 240, and 300 minutes after ^{13}C-glycine administration. The difference of $^{13}CO_2$ concentration ($\Delta^{13}CO_2$) between reference and test breath samples was measured using an infrared $^{13}CO_2$ analyzer, UBit-IR300 (Otsuka Electronics). Body surface area (m^2) of the subjects was calculated[13]; then ^{13}C-cumulative recovery (%) at each time point was calculated. For each subject, CO_2 production per hour (V_{CO2}; mmol/hr) was estimated as 300 × body surface area.[14] ^{13}C-cumulative recovery (%) at the time point t_a was calculated as follows:

$$\text{Cumulative \% recovery } (t_a) = \sum_{t=0}^{t=t_a} \frac{\Delta^{13}CO_2 \times V_{CO_2} \times 0.0112372 \times MW}{Ad \times APE}$$

where MW refers to the molecular weight of ^{13}C-Gly, Ad represents administered dose of ^{13}C-Gly in milligrams, and APR refers to the ^{13}C-enrichment as percentage of atom excess. ^{13}C-cumulative recovery (%) was calculated from administered dose (mg) of ^{13}C-glycine, $\Delta^{13}CO_2$ values (%), body weight (kg), and body length (cm) on the spreadsheet in Excel (Microsoft Corporation, New York, NY; this information is available on request). Differences of means were analyzed statistically by the *t* test using SPSS software version 11.0J (SPSS Japan, Tokyo, Japan). The study was approved by the Ethics Committee of Tohoku University School of Medicine (approval number, 2003-041).

Results

^{13}C-Glycine Oxidation in Control Subjects

To examine the reproducibility, we first performed the breath test five times in the same control subject. Two representative results, designated as tests 1 and 2, are shown in Figure 1B. The peak $\Delta^{13}CO_2$ value was observed at 45 to 60 minutes in test 1 and at 90 to 120

Fig 2. The ^{13}C-glycine breath test in patients with hyperglycinemia. The time-dependent changes of the ^{13}C-cumulative recovery (%) was examined in five glycine encephalopathy (GE) families (A–E) and one family with methylmalonic acidemia (MMA) (F). Dotted lines *indicate the mean and standard deviation in the control subjects. (G) A scattered plot of cumulative recovery (%) within 300 minutes in the control group (n = 10), the GE patients group (n = 5), and the obligate carrier group (n = 7). Mean and standard deviation values of each group are shown as* horizontal lines.

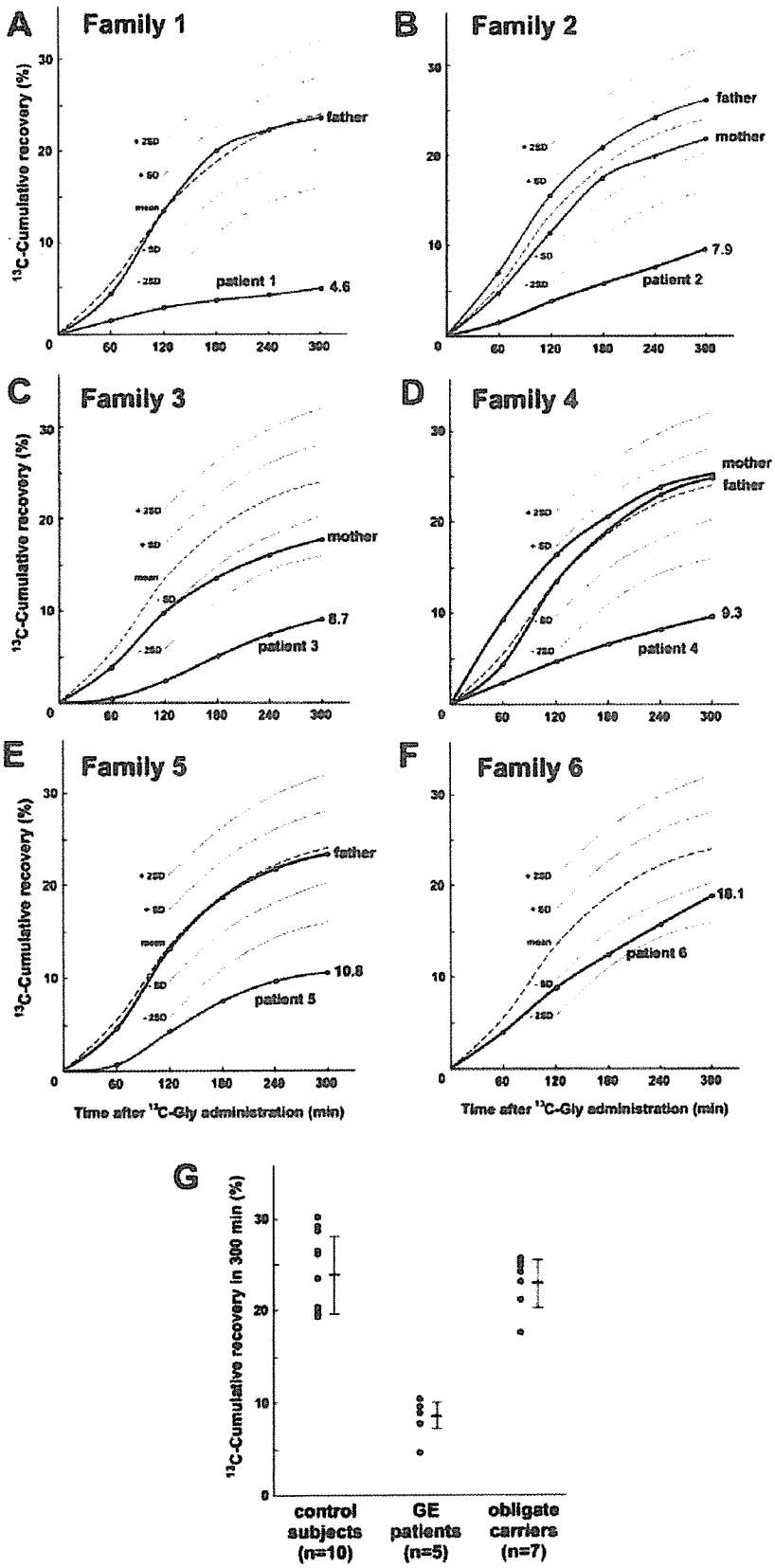
A
Family 1
father
patient 1
4.6
B
Family 2
father
mother
7.9
patient 2
C
Family 3
mother
8.7
patient 3
D
Family 4
mother
father
9.3
patient 4
E
Family 5
father
10.8
patient 5
F
Family 6
18.1
patient 6
+2SD
+SD
mean
-SD
-2SD
^{13}C-Cumulative recovery (%)
Time after ^{13}C-Gly administration (min)
G
^{13}C-Cumulative recovery in 300 min (%)
control subjects (n=10)
GE patients (n=5)
obligate carriers (n=7)

minutes in test 2. This difference in time at the peak $\Delta^{13}CO_2$ value probably reflects variation in gastric emptying between the two tests, because glycine is absorbed in the duodenum but not in the stomach.[15] The ^{13}C-cumulative recovery (%) of tests 1 and 2 is shown in Figure 1C, which suggests that difference of gastric emptying had little effect on the ^{13}C-cumulative recovery at 300 minutes. The mean ± standard deviation of the ^{13}C-cumulative recovery of the same subject in five tests was 21.5 ± 2.0%. The breath test was performed in 10 control subjects: 24.1 ± 4.0% of ^{13}C was recovered within 5 hours after administration of ^{13}C-glycine (see Fig 2). The ^{13}C-glycine breath test was performed previously in neonates for evaluation of gastric emptying time.[16] The ^{13}C-cumulative recovery at 300 minutes after ^{13}C-glycine administration in the reported study was 21.5 ± 4.3% in healthy neonates and 24 ± 4.8% in premature neonates, similar to that in adults and children. We therefore used 24.1 ± 4.0% as the control value in this study.

^{13}C-Glycine Breath Test in Patients with Hyperglycinemia and Their Family Members

The breath test was performed in five patients with GE and their parents (Figs 2A–E). Their mean ^{13}C-cumulative recovery was 8.3 ± 2.3%, which is significantly ($p < 0.001$) less than that in control subjects, and no overlap between the two groups was observed (see Fig 2G). In contrast, the mean ^{13}C-cumulative recovery in the obligate carriers, the parents of the patients, was 23.1 ± 2.9%, which is not significantly ($p = 0.61$) different from the value for the control subjects (see Fig 2G). The ^{13}C-cumulative recovery in the methylmalonic acidemia patient (Patient 6) with secondary hyperglycinemia was 18.1%, which was −1.3 standard deviations less than the mean value (see Fig 2F).

Discussion

We have developed a simple breath test for diagnosis of GE using ^{13}C-glycine and the infrared spectrophotometric $^{13}CO_2$ analyzer. Five GE patients, whose diagnosis of GE was confirmed by mutational analysis, showed significantly less $^{13}CO_2$ excretion than the control subjects, suggesting reliability of the breath test. Previously, $^{13}CO_2$ concentration could be measured only in laboratories equipped with mass-spectrometry facilities and by those possessing expertise. Recently, a simple and inexpensive $^{13}CO_2$ analyzer using infrared spectrophotometry has been developed for the diagnosis of *Helicobacter pylori* infection by the ^{13}C-urea test.[17] Because the analyzer is now distributed widely, the ^{13}C-glycine breath could be readily accomplished in many hospitals and clinics. Recently, we encountered a 1-month-old infant who was suspected to have GE from her typical symptoms and biochemical data. Her parents gave consent for the breath test, but not for the liver biopsy. Her cumulative recovery was 8.7%, enabling the clinical diagnosis of GE rapidly without the invasive liver biopsy or time-consuming mutational analysis.

Patient 5 manifested an atypical clinical course: severe clinical symptoms were observed only for 2 weeks in the neonatal period, but there have been no clinical symptoms thereafter.[18] She is now 12 years old, and her development is normal despite persistence of high plasma and cerebrospinal fluid glycine concentrations. Her exceptionally good prognosis is presumably attributable to the high residual activity of the missense mutation, A802V, which was shown to have 32% residual GLDC activity in the in vitro expression analysis. Low $^{13}CO_2$ excretion was observed in Patient 5, as well as in Patients 1 through 4, suggesting that the test is also useful for the diagnosis of such atypical patients with considerable residual GCS activity.

Patient 6 with methylmalonic acidemia had hyperglycinemia (500–600μM plasma glycine) and showed 18.1% of the cumulative recovery (−1.3 standard deviations) in the breath test. Hyperglycinemia often is associated with organic acidemias. Hayasaka and colleagues[19] analyzed the GCS activity in liver specimens from three hyperglycinemic patients with organic acidemia. One patient, who was metabolically stable while on a low-protein diet, had normal GCS activity in the biopsy of his liver sample. In contrast, two other patients who died with severe metabolic acidosis had markedly reduced hepatic GCS activities. The GCS activity was inhibited by coenzyme A derivatives such as methylmalonyl-coenzyme A and propionyl-coenzyme A, which accumulate in organic acidemias.[20] Because the ^{13}G-glycine breath test is supposed to reflect the GCS activity in vivo, results of the breath test may fluctuate depending on the condition of the patients with organic acidemias.

Patient 1 was a compound heterozygote of a nonsense mutation, Y858X, and a large deletion of the *GLDC* gene, suggesting that he had null residual GCS activity, which is in line with the low value of 4.6% cumulative recovery of Patient 1. Patient 4, in contrast, was compound heterozygous for two missense mutations, N150T and R790W, which showed 14 and 1% residual GLDC activity in the in vitro expression analysis, respectively.[12] Patients 1 and 4 had similar symptoms in neonatal period, but the long-term outcome of Patient 4 was far better. Notably, Patient 4 excreted more $^{13}CO_2$ than Patient 1 in the breath test. Further studies in a larger number of patients are required for verification of the prognostic predictive value of this novel test.

This work was supported by a grant from the Ministry of Education, Culture, Sports, Science, and Technology in Japan. (No. 17591067, S.K.).

We are grateful to the families who participated in this study.

References

1. Kure S, Tada K, Narisawa K. Nonketotic hyperglycinemia: biochemical, molecular, and neurological aspects. J Hum Genet 1997;42:13–22.
2. Hamosh A, Johnston MV. Nonketotic hyperglycinemia. In: Scriver CR, Beaudet AL, Sly WS, Valle D, eds. The metabolic and molecular bases of inherited disease. Vol 2. 8th ed. New York: McGraw-Hill, 2001:2065–2078.
3. Tada K, Kure S. Nonketotic hyperglycinemia: Pathophysiological studies. Proc Japan Acad 2005;81:411–417.
4. Dinopoulos A, Kure S, Chuck G, et al. Glycine decarboxylase mutations: a distinctive phenotype of nonketotic hyperglycinemia in adults. Neurology 2005;64:1255–1257.
5. Flusser H, Korman SH, Sato K, et al. Mild glycine encephalopathy (NKH) in a large kindred due to a silent exonic GLDC splice mutation. Neurology 2005;64:1426–1430.
6. Hoover-Fong JE, Shah S, Van Hove JL, et al. Natural history of nonketotic hyperglycinemia in 65 patients. Neurology 2004; 63:1847–1853.
7. Dinopoulos A, Matsubara Y, Kure S. Atypical variants of nonketotic hyperglycinemia. Mol Genet Metab 2005;86:61–69.
8. Korman SH, Gutman A. Pitfalls in the diagnosis of glycine encephalopathy (non-ketotic hyperglycinemia). Dev Med Child Neurol 2002;44:712–720.
9. Yoshida T, Kikuchi G. Majors pathways of serine and glycine catabolism in various organs of the rat and cock. J Biochem (Tokyo) 1973;73:1013–1022.
10. Koletzko B, Sauerwald T, Demmelmair H. Safety of stable isotope use. Eur J Pediatr 1997;156(suppl 1):S12–S17.
11. Takayanagi M, Kure S, Sakata Y, et al. Human glycine decarboxylase gene (GLDC) and its highly conserved processed pseudogene (psiGLDC): their structure and expression, and the identification of a large deletion in a family with nonketotic hyperglycinemia. Hum Genet 2000;106:298–305.
12. Kure S, Ichinohe A, Kojima K, et al. Mild variant of nonketotic hyperglycinemia with typical neonatal presentations: mutational and in vitro expression analyses in two patients. J Pediatr 2004; 144:827–829.
13. Haycock GB, Schwartz GJ, Wisotsky DH. Geometric method for measuring body surface area: a height-weight formula validated in infants, children, and adults. J Pediatr 1978;93:62–66.
14. Shreeve WW, Cerasi E, Luft R. Metabolism of [2-14C] pyruvate in normal, acromegalic and hgh-treated human subjects. Acta Endocrinol (Copenh) 1970;65:155–169.
15. Maes BD, Ghoos YF, Geypens BJ, et al. Combined carbon-13-glycine/carbon-14-octanoic acid breath test to monitor gastric emptying rates of liquids and solids. J Nucl Med 1994;35: 824–831.
16. Oishi M, Nishida H, Hoshi J. 13C-glycine breath test to measure gastric emptying of neonates. 13C Igaku 1996;7:32–33.
17. Ohara H, Suzuki T, Nakagawa T, et al. 13C-UBT using an infrared spectrometer for detection of Helicobacter pylori and for monitoring the effects of lansoprazole. J Clin Gastroenterol 1995;20(suppl 2):S115–S117.
18. Korman SH, Boneh A, Ichinohe A, et al. Persistent NKH with transient or absent symptoms and a homozygous GLDC mutation. Ann Neurol 2004;56:139–143.
19. Hayasaka K, Narisawa K, Satoh T, et al. Glycine cleavage system in ketotic hyperglycinemia: a reduction of H-protein activity. Pediatr Res 1982;16:5–7.
20. Hayasaka K, Tada K. Effects of the metabolites of the branched-chain amino acids and cysteamine on the glycine cleavage system. Biochem Int 1983;6:225–230.

The Relation between Intracranial and Intraocular Pressures: Study of 50 Patients

Seyed A. Sajjadi, MD,[1] Mohammad H. Harirchian, MD,[2]
Nasim Sheikhbahaei, MD,[1]
Mohammad R. Mohebbi, MD,[1]
Mohammad H. Malekmadani, MD,[3]
and Hooshang Saberi, MD[4]

Objective: We evaluated the correlation between intracranial (ICP) and intraocular pressure (IOP).

Methods: Of the 77 patients who underwent a lumbar puncture, 27 were excluded secondary to a history of glaucoma, using drugs effective on IOP, and abnormal funduscopic examination. ICP was measured by lumbar puncture. IOP was measured by two scales of Schiotz tonometer in both eyes, and the mean was calculated.

Results: We found a significant correlation between ICP and mean IOP ($p < 0.001$; $r = 0.955$). Body mass index, age, and disease type had no significant effect on this correlation.

Interpretation: IOP is correlated with ICP.

Ann Neurol 2006;59:867–870

Intracranial pressure (ICP) measurement is potentially useful in many clinical situations and has a profound influence on outcome. Rise in ICP may stem from traumatic brain injury, mass effect from tumors, or various hemorrhagic catastrophes.[1] Clinical conditions in which the measurement of ICP noninvasively would be useful include: head trauma, if there is a risk for brain edema; altered or fluctuating levels of consciousness; arrested or progressive hydrocephalus; suspected ventriculoperitoneal shunt blockage; and suspected meningitis before lumbar puncture (LP).[2] Currently, the criterion standard for monitoring of ICP is the

From the [1]School of Medicine and Departments of [2]Neurology, [3]Ophthalmology, and [4]Neurosurgery, Tehran University of Medical Sciences, Tehran, Iran.

Received Nov 25, 2005, and in revised form Feb 24, 2006. Accepted for publication Mar 10, 2006.

The study was performed at Imam General Hospital and Shariati General Hospital affiliated with Tehran University of Medical Sciences, Tehran, Iran. The study was first presented at the 13th Meeting of the European Neurological Society, Istanbul, Turkey, June 14–18, 2003.

Published online Apr 24, 2006, in Wiley InterScience (www.interscience.wiley.com). DOI: 10.1002/ana.20856

Address correspondence to Dr Sajjadi, Blackpool Victoria Hospital, Whinney Heys Road, Blackpool, Lancashire, FY3 8NR United Kingdom. E-mail: s.a.sajjadi@doctors.org.uk

J Hum Genet (2006) 51:455–460
DOI 10.1007/s10038-006-0384-7

ORIGINAL ARTICLE

**Fumiaki Kamada · Shigeo Kure · Takayuki Kudo
Yoichi Suzuki · Takeshi Oshima · Akiko Ichinohe
Kanako Kojima · Tetsuya Niihori · Junko Kanno
Yoko Narumi · Ayumi Narisawa · Kumi Kato
Yoko Aoki · Katsuhisa Ikeda · Toshimitsu Kobayashi
Yoichi Matsubara**

A novel *KCNQ4* one-base deletion in a large pedigree with hearing loss: implication for the genotype–phenotype correlation

Received: 18 November 2005 / Accepted: 23 January 2006 / Published online: 5 April 2006

Abstract Autosomal-dominant, nonsyndromic hearing impairment is clinically and genetically heterogeneous. We encountered a large Japanese pedigree in which nonsyndromic hearing loss was inherited in an autosomal-dominant fashion. A genome-wide linkage study indicated linkage to the DFNA2 locus on chromosome 1p34. Mutational analysis of *KCNQ4* encoding a potassium channel revealed a novel one-base deletion in exon 1, c.211delC, which generated a profoundly truncated protein without transmembrane domains (p.Q71fsX138). Previously, six missense mutations and one 13-base deletion, c.211_223del, had been reported in *KCNQ4*. Patients with the *KCNQ4* missense mutations had younger-onset and more profound hearing loss than patients with the 211_223del mutation. In our current study, 12 individuals with the c.211delC mutation manifested late-onset and pure high-frequency hearing loss. Our results support the genotype–phenotype correlation that the *KCNQ4* deletions are associated with later-onset and milder hearing impairment than the missense mutations. The phenotypic difference may be caused by the difference in pathogenic mechanisms: haploinsufficiency in deletions and dominant-negative effect in missense mutations.

Keywords DFNA2 · *KCNQ4* · Linkage · Mutation · Haploinsufficiency

F. Kamada · S. Kure (✉) · T. Kudo · Y. Suzuki · A. Ichinohe
K. Kojima · T. Niihori · J. Kanno · Y. Narumi · A. Narisawa
K. Kato · Y. Aoki · Y. Matsubara
Department of Medical Genetics,
Tohoku University School of Medicine,
1-1 Seiryo-machi, Aoba-ku,
Sendai 980-8574, Japan
E-mail: skure@mail.tains.tohoku.ac.jp
Tel.: +81-22-7178140
Fax: +81-22-7178142

T. Oshima · K. Ikeda · T. Kobayashi
Department of Otorhinolaryngology, Head and Neck Surgery,
Tohoku University School of Medicine, Sendai, Japan

F. Kamada · S. Kure · K. Kato · Y. Aoki · Y. Matsubara
21st COE Program "Comprehensive Research and Education Center for Planning of Drug Development and Clinical Evaluation", Tohoku University, Sendai, Japan

Introduction

Hearing impairment is one of the most common communication disorders in humans and is both clinically and genetically heterogeneous. Approximately 1 in 1,000 children is affected by hearing impairment (Morton 1991), and in half of the cases genetic factors are involved (Marazita et al. 1993). Nonsyndromic hearing impairment is classified according to its mode of inheritance as DFNA, DFNB, and DFN (autosomal dominant, autosomal recessive, and X-linked, respectively). Currently, 54 autosomal dominant, 59 autosomal recessive, and 8 X-linked loci associated with nonsyndromic hearing impairment have been mapped (Hereditary Hearing Loss Homepage, http://webhost.ua.ac.be/hhh/). A total of 21 DFNA genes have been reported to date. Several of the genes are involved in both dominant and recessive deafness (*GJB2*, *GJB6*, *MYO6*, *MYO7A*, *TECTA* and *TMC1*). For example, a null *GJB2* mutation, 35delG in Caucasians and 235delC in Asians, is responsible for the majority of autosomal recessive sensorineural deafness in the respective populations (Kenneson et al. 2002; Kudo et al. 2000; Usami et al. 2002). In contrast, some *GJB2* mutations, including R75W, segregate with deafness in an autosomal-dominant fashion (Richard et al. 1998). The dominant-negative effect of the R75W mutation was suggested by the transgenic expression in mice (Kudo et al. 2003).

DFNA2 is a locus responsible for autosomal-dominant, nonsyndromic hearing impairment in chromosome 1p34 (Coucke et al. 1994; Van Camp et al. 1997). Two

hearing impairment genes, *GJB3* and *KCNQ4*, have been identified in the DFNA2 locus (Kubisch et al. 1999; Xia et al. 1998). The *KCNQ4* gene consists of 14 exons that encode a protein of 695 amino acids (MIM*603537). The KCNQ4 protein contains six transmembrane domains and a P-loop region that forms the potassium-selective channel pore (Kubisch et al. 1999). Six missense mutations have been reported in the *KCNQ4* gene to date (Akita et al. 2001; Coucke et al. 1999; Kubisch et al. 1999; Talebizadeh et al. 1999; Topsakal et al. 2005; Van Camp et al. 2002; Van Hauwe et al. 2000). Co-expression studies in *Xenopus* oocytes revealed that the mutant channel protein with a missense mutation exerted a strong dominant-negative effect, which may explain the autosomal-dominant inheritance of *KCNQ4* deafness (Kubisch et al. 1999). Besides the missense mutations, one small deletion has also been reported (Coucke et al. 1999). Because the mutation generated a channel protein that is truncated before the first transmembrane domain, it is unlikely that the mutant protein had a dominant-negative effect. The pathogenic mechanism of this deletion in *KCNQ4*, therefore, remains elusive (Coucke et al. 1999). Recently, Topsakal et al. (2005) noted a phenotypic difference among eight pedigrees with six missense mutations and a single pedigree with the c.211_223del mutation. Based on these data, a hypothesis for the genotype–phenotype correlation is suggested in which younger-onset and all-frequency hearing loss is associated with missense mutations, and later-onset and pure high-frequency hearing loss with null mutations. Although it is an attractive hypothesis, more phenotypic information should be accumulated from individuals with other null *KCNQ4* mutations in order to evaluate the genotype–phenotype correlation.

We identified a novel one-base deletion in *KCNQ4* exon 1 in a large Japanese pedigree with hearing loss using genome-wide linkage analysis and candidate gene analysis. Individuals with the deletion manifested later-onset and pure high-frequency hearing loss, compared with reported patients with *KCNQ4* missense mutations. Our observations support the phenotype–genotype correlation in *KCNQ4* deafness, and suggest that haploinsufficiency is the most likely mechanism for development of hearing loss caused by the null *KCNQ4* mutations.

Materials and methods

Family data

A Japanese family affected with autosomal-dominant, nonsyndromic hearing impairment was identified (Fig. 1). All affected family members had an affected and an unaffected parent, and four male-to-male transmissions were noted. Twenty-four members of the family participated in this study after giving informed consent. They were asked to complete a questionnaire to exclude other causes of hearing impairment. Special attention was paid to features that might have caused syndromic hearing impairment. All participants underwent otoscopic and audiological examinations. Pure-tone audiograms were obtained in a sound-treated room. Air conduction thresholds were measured in dB hearing level (HL) at 500, 1,000, 2,000, 4,000, and 8,000 Hz. Diagnosis of progressive sensorineural hearing impairment was based on pure-tone audiogram, questionnaire information, and medical records. Family members were considered to be affected if they had sensorineural hearing impairment of more than 25 dB at more than one frequency. Syndromic hearing impairment and environmental causes of deafness were excluded from this study. The ethics committee of Tohoku University School of Medicine approved this study.

Genetic analysis

Blood samples were obtained from 24 family members, 13 affected and 11 unaffected. Control samples were obtained from 100 Japanese subjects with normal hearing. DNA was extracted from peripheral blood leukocytes using the Genomic DNA purification kit (Promega, Madison, WI, USA). In the genome-wide linkage analysis, microsatellite markers of the Human MAPPAIRS (Invitrogen, Carlsbad, CA, USA) were used for genotyping on the ABI 373A DNA Sequencer. Detailed information for additional genetic markers used in this study can be found in the NCBI Human Map Viewer. We performed pedigree and haplotype constructions using the Cyrillic version 2.1 software. Two-point LOD scores were calculated by the MLINK program of the LINKAGE version 5.1 software package (Lathrop et al. 1984). The affected allele frequency and penetrance were set at 0.0001 and 1.0, respectively. Multipoint linkage analyses were conducted using the GENEHUNTER 2 (Kruglyak et al. 1996).

Mutation analysis was performed by genomic exon sequencing. PCR was carried out using primers flanking 1 *GJB3* exon and 14 *KCNQ4* exons. Reaction conditions were optimized for different primer sets. Primer sequences were based on the genomic sequence available in the Genbank (*GJB3*, AF099730; *KCNQ4*, AH007377). The amplification products from both genes were sequenced with the ABI Prism BigDye Terminator Cycle Sequencing Ready Reaction Kit (Applied Biosystems, Foster City, CA, USA) on the ABI 310 Genetic Analyzer and analyzed using the ABI DNA Sequencing Analysis version 5.1 software.

Results

Genetic analysis

In the genome-wide screening, a maximum two-point LOD score of 5.42 at $\theta = 0$ was obtained for GATA129H04 (penetrance = 1.0, Table 1). In addition, multipoint linkage analysis with GATA129H04 revealed

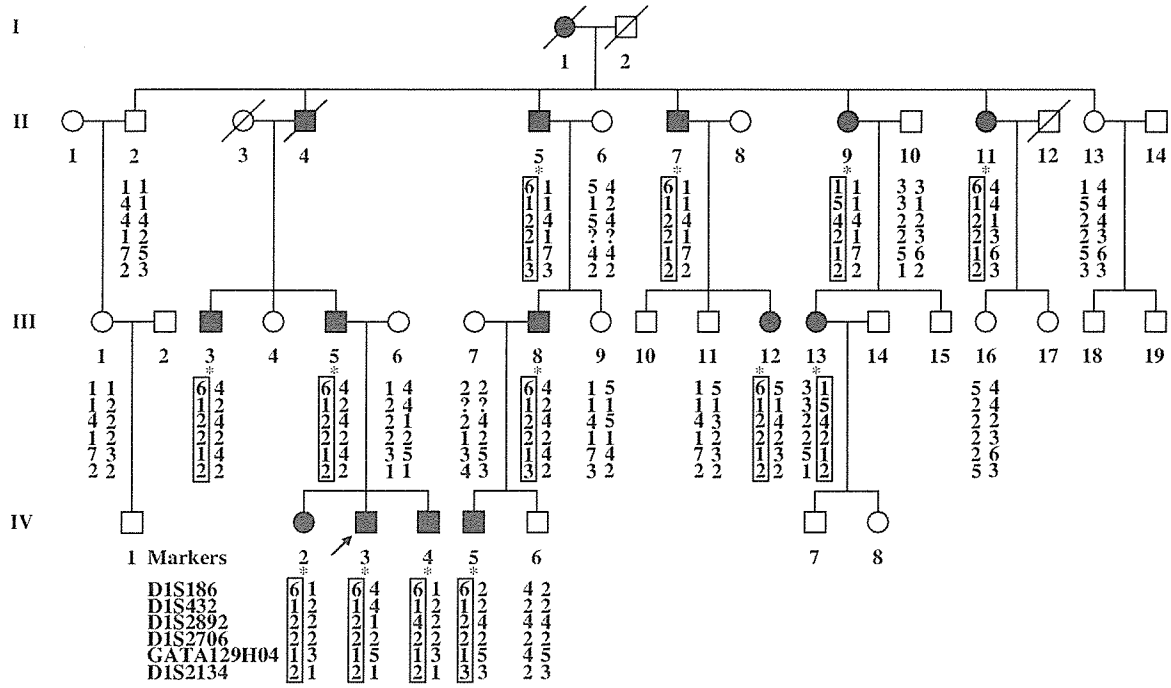

Fig. 1 Pedigree of the Japanese family with nonsyndromic, autosomal-dominant hearing impairment. The *asterisks* indicate those individuals in whom a *KCNQ4* mutation was identified. The haplotype *enclosed in the box* shows the disease haplotype

Table 1 Two-point LOD scores for linkage between hearing impairment and microsatellite markers in a Japanese family

Marker	Marshfield map distance (cM)	LOD score at θ					
		0	0.05	0.1	0.2	0.3	0.4
D1S234	55.10	2.99	2.75	2.49	1.93	1.28	0.59
D1S496	64.38	−999.99	3.09	3.00	2.44	1.64	0.71
D1S186	67.22	−999.99	3.09	2.97	2.35	1.50	0.55
D1S432	69.86	−999.99	0.81	1.13	1.15	0.86	0.44
D1S2892	70.41	−999.99	−1.59	−0.69	−0.10	0.02	0.02
D1S2706	71.13	1.68	1.53	1.38	1.04	0.66	0.25
GATA129H04	72.59	5.42	4.97	4.50	3.48	2.32	1.01
D1S2134	75.66	−999.99	0.73	0.83	0.70	0.45	0.20
D1S200	82.41	−999.99	3.16	3.02	2.36	1.47	0.50

a maximum nonparametric linkage (NPL) score of 10.95 (data not shown). This marker is known to flank the DFNA2 locus on chromosome 1p34. As shown in Fig. 1, the most likely haplotypes were constructed to determine the borders of the critical region. All affected family members shared the same disease haplotype. The recombination between D1S2134 and the gene for hearing impairment was found in family member II-5. In family member II-9, recombination occurred between the gene for hearing impairment and marker D1S2892. These events localized the gene for hearing impairment between D1S2892 and D1S2134. This region is at 1p34, where the DFNA2 locus resides. These data clearly indicated linkage of the hearing impairment to the DFNA2 locus in this family.

As linkage to the DFNA2 locus was proven in this family, both *GJB3* and *KCNQ4* genes were examined for mutations. First, we sequenced the coding region of *GJB3* in this family, but did not find any mutations. Subsequently, we analyzed all *KCNQ4* exons. In exon 1 we identified a deletion of C at nucleotide position 211 of the *KCNQ4* cDNA sequence (Fig. 2). All affected family members were heterozygous for this mutation (Fig. 1). The mutation was not detected in the 100 normal controls.

Clinical features

We performed a clinical study on the Japanese family members (13 affected) with a null *KCNQ4* mutation to delineate its phenotypic features (Table 2). Patients showed a nonsyndromic, postlingual, symmetric and sensorineural hearing impairment. The hearing impair-